ATP activates non-selective cation channels and calcium release in inner hair cells of the guinea-pig cochlea

Masashi Sugasawa, Carlos Erostegui, Christophe Blanchet and Didier Dulon*

Laboratoire d'Audiologie Expérimentale, INSERM et Université de Bordeaux II, Hôpital Pellegrin, 33076 Bordeaux, France

1. ATP-evoked currents and Ca^{2+} signals were simultaneously recorded in isolated inner hair cells (IHC) of guinea-pig cochlea by combining conventional whole-cell or perforated patch clamp recording with indo-1 dual emission microfluorometry.

2. In most IHCs, voltage clamped near resting membrane potential (−40 mV), extracellular ATP evoked a rapid inward current (time constant, 150 ms). This current was concomitant with a slow rise in $[Ca^{2+}]_i$ (time constant, 5 s). The ATP-evoked inward currents could be repeated several times with only a small run-down in amplitude (< 10%), while the ATP-evoked Ca^{2+} responses showed a rapid run-down (> 80% at the third ATP application).

3. The current–voltage relationship of ATP-evoked currents showed a reversal potential at -11 ± 6 mV ($n = 8$), suggesting that ATP essentially activated a non-specific cationic conductance. On the contrary, the amplitude of the ATP-evoked Ca^{2+} responses did not show significant dependence on holding membrane potential.

4. The Ca^{2+} response showed an apparent K_d for ATP (EC_{50}, $1{\cdot}8 \pm 0{\cdot}3$ μM; Hill coefficient, $1{\cdot}0 \pm 0{\cdot}1$) eightfold smaller than for the evoked currents (EC_{50}, $13{\cdot}7 \pm 3{\cdot}0$ μM; Hill coefficient, $2{\cdot}0 \pm 0{\cdot}7$).

5. Perfusion with high extracellular Ca^{2+} solution (10 mM $CaCl_2$) reduced the amplitude of the ATP-evoked currents by 90%, while perfusion with zero Ca^{2+} solution increased it by more than 100%. However, similar variations in external Ca^{2+} concentration did not change the amplitude of the ATP-evoked Ca^{2+} responses. Furthermore, intracellular heparin (1 mg ml^{-1}), a potent inhibitor of $InsP_3$ receptors, did not significantly change the amplitude of ATP-evoked currents but reduced the ATP-evoked Ca^{2+} response, suggesting again that the latter is related to Ca^{2+} release from intracellular stores.

6. The results suggested that two types of P_2-purinergic receptor are expressed in IHCs: ATP-gated ion channels and ATP-activated metabotropic receptors. At submicromolar ATP concentrations, the metabotropic receptors raising intracellular $[Ca^{2+}]$ would hyperpolarize IHCs via Ca^{2+}-sensitive K^+ channels. The ATP-gated ion channels activated at higher ATP concentrations would mainly have a depolarizing effect on IHCs.

There is recent evidence that extracellular ATP modifies sound-evoked responses in the cochlea (Kujawa, Erostegui, Fallon, Crist & Bobbin, 1994) and several cellular studies *in vitro* have shown that almost all cells of the organ of Corti, both supporting and sensory hair cells, are possible targets for the action of ATP (Ashmore & Ohmori, 1990; Nakagawa, Akaike, Kimituki, Komune & Arima, 1990; Dulon, Mollard & Aran, 1991*a*; Dulon, Moataz & Mollard, 1993). This widespread cellular action of ATP renders the precise role of ATP in the physiology of the cochlea difficult to understand.

Extracellular ATP is well known for being implicated in various other precise physiological processes by activating specific membrane receptors. These receptors have been defined as P_2-purinergic receptors allowing ATP to act as a potential neurotransmitter or neuromodulator (Burnstock, 1978; Dubyak & El-Moatassim, 1993). Two main P_2-purinergic receptor families have been described in excitable and non-excitable cells: (i) ATP-gated non-specific cationic channels (P_{2X}) which have been recently cloned and sequenced from neurons and smooth muscle (Valera *et al.* 1994; Brake, Wagenbach & Jullius, 1994); (ii) ATP-

* To whom correspondence should be addressed.

activated receptors coupled to G-proteins, defined as metabotropic receptors (P_{2Y}), triggering Ca^{2+} release from intracellular stores (for review see Dubyak & El-Moatassim, 1993).

In both supporting and hair cells of the cochlea, the presence of these two types of purinergic receptor have been suggested by studies using either Ca^{2+} spectrofluorometry technology (Ashmore & Ohmori, 1990; Dulon *et al.* 1991*a*, 1993; Nilles, Järlebark, Zenner & Heilbronn, 1994) or electrophysiological whole-cell membrane current recording (Nakagawa *et al.* 1990). Although Ashmore & Ohmori (1990) simultaneously recorded ATP-evoked Ca^{2+} responses and current in outer hair cells (OHCs), there is no quantitative study which has extensively combined both patch clamp recording and Ca^{2+} measurement to characterize ATP responses. Therefore, the relationship between the two types of P_2-purinergic receptor expressed in the same cochlear cell type remains unclear.

It has been previously shown that extracellular ATP increases $[Ca^{2+}]_i$ in isolated inner hair cells (IHCs) with probable involvement of metabotropic receptors (Dulon *et al.* 1991*a*), but also activates ionotropic receptors (Housley, Greenwood, Mockett, Muñoz & Thorne, 1993). The aim of the present study was to characterize, by simultaneously measuring ATP-evoked membrane currents and changes in intracellular calcium ($[Ca^{2+}]_i$), the metabotropic and ionotropic purinergic responses coexisting in IHCs. We have considered IHCs in the present study because they are the main transducers in the cochlea (for review see Dallos, 1992). Indeed, the IHCs contact the majority of the afferent nerve fibres sending acoustic information to the brainstem (Kiang, Rho, Northrop, Liberman & Ryugo, 1982). Cellular characterization of ATP-evoked Ca^{2+} signals and membrane currents would be important to determine the receptor families involved in IHCs and would be helpful for elucidating their physiological roles in the cochlea.

METHODS

Preparation of IHCs

IHCs were isolated as previously described (Dulon, Zajic & Schacht, 1991*b*; Dulon, Sugasawa, Blanchet & Erostegui, 1995). Pigmented guinea-pigs with positive Preyer's reflex and body weight of 200–300 g were deeply anaesthetized with a 0·5 ml intramuscular injection of a solution consisting of 1 volume of 50 mg ml^{-1} ketamine hydrochlorate (Ketalar; Parke-Davis, Courbevoie, France) and 1 volume of 2% xylazine (Rompun; Bayer, Leverkusen, Germany). The animals were then decapitated and the temporal bones were quickly removed. After removal of the bony shell of the cochlea, the organ of Corti was dissected with a fine metal probe and transferred to Hank's balanced salt solution (HBSS) containing (mM): $CaCl_2$, 1·25; $MgSO_4$, 0·81; KCl, 5·4; KH_2PO_4, 0·44; NaCl, 136·9; NaH_2PO_4, 0·34; D-glucose, 5·5; buffered with 5 mM Hepes (*N*-2-hydroxyethylpiperazine-*N*′-2-ethanesulphonic acid); pH was adjusted to 7·40 with NaOH and osmolality to 300 mosmol (kg water)$^{-1}$ with 4 N NaCl, increasing NaCl concentration to less than 141 mM. After enzymatic treatment with collagenase (0·5 mg ml^{-1}; Type IV, Sigma) for 20 min and trypsin (0·05 mg ml^{-1}; Type III, Sigma) for 10 min at room temperature (20–25 °C), the pieces of organ of Corti were transferred to several dishes containing 50 μl HBSS. The cells were mechanically dissociated by gentle flow through a micropipette (Gilson, France). Finally, the cells were incubated for 20 min in a humid chamber and rinsed with 1–2 ml HBSS. The dish was placed on an inverted microscope (Nikon Diaphot) with Hoffman modulation phase-contrast optics.

The care and use of guinea-pigs in this study was approved by the French Ministry of Agriculture in agreement with EEC regulations.

Identification of IHCs

The morphological characteristics used to distinguish IHCs from OHCs in our preparation have been previously described (Dulon *et al.* 1991*b*; Dulon *et al.* 1995). Typically, isolated IHCs are pear-shaped cells, 30–40 μm in length, which have a characteristically tilted cuticular plate, aligned stereocillia, and centrally located nucleus. IHCs have a typical resting membrane potential of −50 mV, while OHC resting potentials are around −70 mV. Cells presenting large swelling with Brownian movements within their cytoplasm, low membrane birefringence, resting membrane potential above −30 mV or high resting $[Ca^{2+}]_i$ (> 400 nM) were discarded.

Electrical recording

Inner hair cells were either recorded under conventional whole-cell voltage clamp (number of cells (n) = 74) (Hamill, Marty, Neher, Sakmann & Sigworth, 1981) or under perforated patch configuration (n = 23) (Horn & Marty, 1988). Patch electrodes were pulled from borosilicate glass (GC150TF-10; Clark Electromedical Instruments, Pangbourne, UK) using a Sachs–Flaming micropipette puller (model PC-84; Sutter Instruments, Navato, CA, USA). In conventional whole-cell recordings, the electrodes were backfilled with internal solution containing (mM): KCl, 150; $MgCl_2$, 2; Hepes, 5; BAPTA (1,2-bis(*O*-aminophenoxy)ethane-*N*,*N*,*N*′,*N*′-tetraacetic acid), 1; pH was adjusted to 7·2 with KOH and osmolality to approximately 300 mosmol (kg water)$^{-1}$ with glucose. In perforated patch conditions, nystatin was dissolved in dimethyl sulphoxide at a concentration of 20 mg ml^{-1}. This stock solution was freshly diluted to a final concentration of 200 μg ml^{-1} in the following solution (mM): KCl, 150; $MgCl_2$, 2; Hepes, 5; pH was adjusted to 7·2 with KOH and osmolality to approximately 300 mosmol (kg water)$^{-1}$ with glucose. The resistance of the pipettes ranged from 4 to 5 MΩ.

The voltage clamp recordings were obtained using a Bio-logic RK-400 amplifier (Bio-logic Science Instruments, Claix, France) coupled to an analog-to-digital converter (DMA; Scientific Solutions Inc., Solon, OH, USA) and to a 486DX2 microcomputer. All records were low-pass filtered at 10 kHz with a 5-pole Bessel filter and no leak current correction was made. The voltage ramp protocol and analysis shown in Fig. 2*A* were performed using pCLAMP software (Axon Instruments Inc., Foster City, CA, USA). The data presented in all other figures were collected using Axotape software (Axon Instruments Inc.). The junction potentials were corrected prior to each recording. For conventional whole-cell or perforated recordings, respectively, series resistance averaged 18·5 ± 0·9 (n = 74) or 40·3 ± 4·9 MΩ (n = 23), cell input resistance (at a holding potential (V_h) of −40 mV) was 230 ± 20 or 410 ± 60 MΩ, membrane capacitance was 8·3 ± 0·5 or

11·4 ± 2·0 pF. In all figures, holding membrane potentials were corrected for voltage drop across pipette series resistance after data collection. All experiments were carried out at room temperature (20–25 °C).

Ca^{2+} measurement with indo-1

In conventional whole-cell recording, IHCs were loaded with 50 μM indo-1 via the patch pipette, while in perforated patch conditions, the cells were pre-incubated with 2 μM indo-1 AM at room temperature (20–25 °C) for 30 min. Intracellular calcium concentration ($[Ca^{2+}]_i$) was monitored by dual emission microspectrofluorometry at 405 and 480 nm as previously described (Dulon *et al.* 1991*a*, 1995). The two emission signals were divided on-line giving the emission fluorescence ratio R (ratio of fluorescence at 405 and 480 nm, F_{405}/F_{480}) which was recorded using Axotape software. Calibration and calculation of $[Ca^{2+}]_i$ from the ratios were performed as previously reported (Dulon *et al.* 1991*a*).

Drug delivery

During the experiments, the cells were continuously perfused with HBSS at 150–200 μl min^{-1}. The drugs were applied to IHCs using a conventional U-tubing system (Murase, Ryu & Randic, 1989). The tip of the ejection pipette had a diameter of 100 μm and was placed about 500 μm away from the cells. The delivery time constant was estimated to be 100 ms by measuring the time needed to change the junction potential of a recording patch electrode when applying a 100 mM KCl solution.

In experiments in which rapid kinetic analysis was needed, as shown in Fig. 8, ATP was applied to the cells by using a pressure puff-ejector system (Picospritzer II; General Valve Corp., Fairfield, NJ, USA) via a glass pipette with a tip size similar to that of the patch electrode. This puff electrode was placed at about 10–20 μm away from the cells and drug delivery time was determined to range between 10 and 20 ms.

In normal HBSS conditions, although ATP exists primarily as a complex with the divalent cations Mg^{2+} (MgATP) and Ca^{2+} (CaATP) in the figures it will be referred to simply as ATP. Free ATP concentration was calculated using MAXC software (courtesy of Dr Chris Patton, Hopkins Marine Station, Standford University, CA, USA).

Data are expressed as means ± S.E.M. Statistical comparisons were made using Student's unpaired t test.

Chemicals and drugs

Indo-1, indo-1 AM and ionomycin were purchased from Calbiochem. All other reagents were obtained from Sigma.

RESULTS

Resting membrane potential and $[Ca^{2+}]_i$

In conventional whole-cell recording, zero current membrane potential (resting potential) of isolated IHCs reached a stable value at −52·4 ± 0·9 mV ($n = 74$) within 5 min of rupturing the patch membrane. A similar resting membrane potential of −46·2 ± 2·7 mV ($n = 23$) was obtained in perforated patch conditions. This resting potential was similar to those previously reported by intracellular recordings *in vivo* (Dallos, 1986) and by whole-cell patch clamp recordings in isolated IHCs (Gitter & Zenner, 1990; Dulon *et al.* 1991*a*) but was somewhat smaller than the value measured in clustered IHCs reported by Kros & Crawford (1990).

Immediately after rupturing the patch membrane in the whole-cell configuration, $[Ca^{2+}]_i$ was generally high (> 600 nM) but progressively decreased to a steady-state value within 5 min of intracellular dialysis with the internal solution. $[Ca^{2+}]_i$ in the steady state ranged from 100 to 400 nM (mean, 230 ± 24 nM; $n = 32$) for IHCs perfused in standard HBSS. The initial high value of $[Ca^{2+}]_i$ might be due to calcium contamination at the tip of the patch pipette before seal formation or to a transient Ca^{2+} influx after rupturing the seal. In perforated patch conditions with IHCs loaded using indo-1 AM, there was no initial rise in resting $[Ca^{2+}]_i$ which averaged 180 ± 18 nM ($n = 19$). This was not significantly different from the whole-cell recording condition.

Extracellular ATP increased $[Ca^{2+}]_i$ and activated membrane currents

Extracellular application of 10 μM ATP via the U-tubing system evoked a large inward current (238 ± 32 pA; $n = 53$) in IHCs voltage clamped at −40 mV (near resting membrane potential) (Fig. 1*A*). As measured in four different cells using the puff pressure-ejection system allowing fast drug delivery, the activation kinetic of the inward current evoked by 10 μM ATP at a V_h of −40 mV could be well fitted by a single exponential function with a mean time constant (τ) of 150 ± 20 ms. In cells in which both $[Ca^{2+}]_i$ and electrical measurements were simultaneously measured ($n = 13$ in perforated patch and $n = 32$ in whole-cell patch), the ATP evoked-current was accompanied by a rise in $[Ca^{2+}]_i$ (Fig. 1*A*). The overall Ca^{2+} response in both recording conditions showed a slow kinetic with a mean τ of 5·0 ± 0·9 s and peaked with a large delay of 6·2 ± 0·3 s with the peak of the corresponding inward current. The peak of the Ca^{2+} response for 10 μM ATP corresponded to a mean increment in $[Ca^{2+}]_i$ of 113 ± 16 nM in the perforated patch configuration and to 76 ± 20 nM in the whole-cell configuration. The amplitude of the Ca^{2+} response was not significantly different between the two recording conditions.

The Ca^{2+} responses showed large and rapid run-down decreasing by more than 80% after three ATP applications (Fig. 1*A* and *C*). This run-down was observed in both perforated patch and whole-cell conditions suggesting that it was not due to intracellular dialysis. Even if the cells were rinsed for more than 15 min after ATP application, no recovery of the original Ca^{2+} response was observed. On the contrary, the ATP-evoked inward current showed little run-down (< 10%) with respect to its peak amplitude after several successive ATP applications (Fig. 1*A* and *C*) but showed a marked difference in its kinetic of inactivation. Indeed, the ATP current displayed a slower inactivation after several ATP applications suggesting the involvement of another labile opposite current (see discussion below).

The ATP-evoked current was biphasic in some cells (Fig. 1*B*). This biphasic response was clearly observed in three of thirty-three cells (9·1 %) in the conventional whole-cell configuration and in nine of twenty cells (45 %) in the perforated patch configuration. There was no significant difference betweeen the amplitudes of the Ca^{2+} response in cells showing a clear biphasic current and cells with no biphasic current. However, similar to the Ca^{2+} response, this secondary activated current, which was outward directed at potentials near rest, showed a slow kinetic of activation with a mean τ of 4·4 ± 0·9 s and a rapid run-down after several applications of ATP. This secondary activated ATP outward current might be due to Ca^{2+}-activated K^+ channels which have recently been suggested to be present in IHCs (Housley *et al.* 1993; Dulon *et al.* 1995). The absence of a clear biphasic current response in most IHCs does not exclude the possibility that Ca^{2+}-activated K^+ currents were not activated in these cells. In most IHCs, the inactivation kinetic of the ATP-evoked inward current decreased after several ATP applications suggesting the participation of an opposite current (presumably Ca^{2+}-activated K^+ currents) upon the first ATP-evoked response and this opposite current showed a strong run-down occurring in parallel to the Ca^{2+} response (Fig. 1*A*).

The higher rate of ATP-evoked biphasic current observed in the perforated patch configuration indicates that some essential factor probably deteriorates more rapidly or is inactivated under conventional whole-cell recording. This difference was unlikely to have been due to a difference in intracellular Ca^{2+} buffering between the two recording configurations because 1 mM BAPTA, used here in the whole-cell configuration, has been shown in saccular hair cells to be equivalent to the natural Ca^{2+} buffer regarding the activation of Ca^{2+}-activated K^+ channels (Roberts, 1993).

It is also interesting to note that ATP-activated Ca^{2+}-dependent K^+ currents were also shown to be sensitive to electrophysiological recording conditions and were only observed in the perforated patch configuration in mouse macrophages and neurons (Hara, Ichinose, Sawada & Maeno, 1990; Ueno, Ishibashi & Akaike, 1992). Furthermore, the conventional whole-cell configuration has been suggested to affect membrane excitability more rapidly than perforated patch conditions, especially Ca^{2+}-mediated responses (Marty & Neher, 1985). Our observations suggested that ATP-evoked Ca^{2+} responses might normally trigger Ca^{2+}-activated outward K^+ currents in IHCs *in vivo*, leading therefore to hyperpolarization from rest.

Influence of membrane potential on ATP-evoked responses

The current–voltage (*I–V*) relationship of ATP evoked-current is shown in Fig. 2*A*. In whole-cell configuration, IHCs were depolarized from −80 to 40 mV by a ramp protocol of 1·2 mV ms^{-1} during continuous application of 10 μM ATP. The *I–V* curve was linear at negative

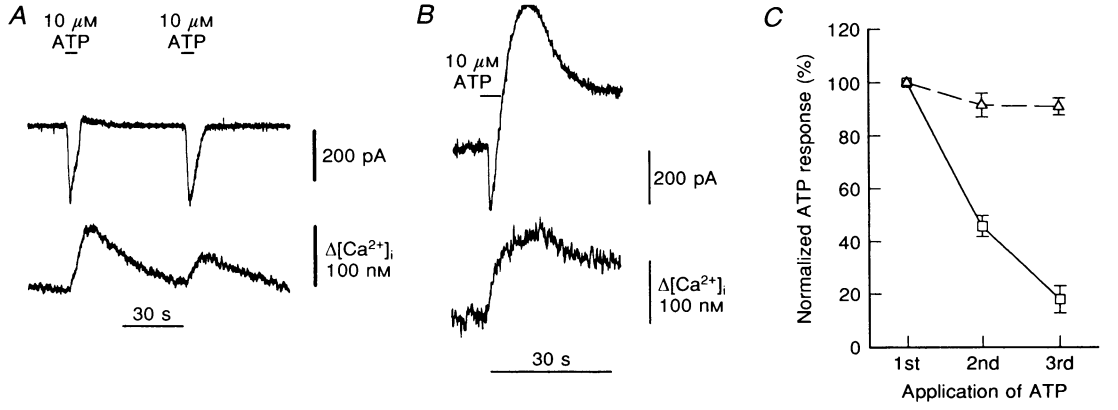

Figure 1. Simultaneous recording of ATP-evoked currents and rise in $[Ca^{2+}]_i$

A, ATP (10 μM) evoked a rapid inward current (upper trace) followed by a small overshoot on first application of ATP. The ATP-evoked inward current had a similar amplitude after a second ATP application, while the overshoot response disappeared. The Ca^{2+} response (lower trace), showing a slower activation kinetic, demonstrated a large run-down (> 50 %) on second application of ATP. Note the 10 s delay between the inward current and Ca^{2+} response peaks. *B*, ATP evoked a biphasic current. The early inward current was followed by a large outward current (presumably Ca^{2+}-activated K^+ current). Note that the outward current was parallel to the rise in $[Ca^{2+}]_i$. The recordings shown in *A* and *B* were obtained from two different IHCs voltage clamped near resting membrane potential at −40 mV using the conventional whole-cell technique. *C*, the relative amplitude of the Ca^{2+} responses (□) and inward currents (△) after first, second and third applications of 10 μM ATP are plotted. The Ca^{2+} responses showed large run-down while the inward current responses were essentially unaffected after successive ATP applications. The mean values were from 10 IHCs. Here and in subsequent figures, bars represent ± S.E.M. and ATP responses are normalized to the first ATP response for each cell.

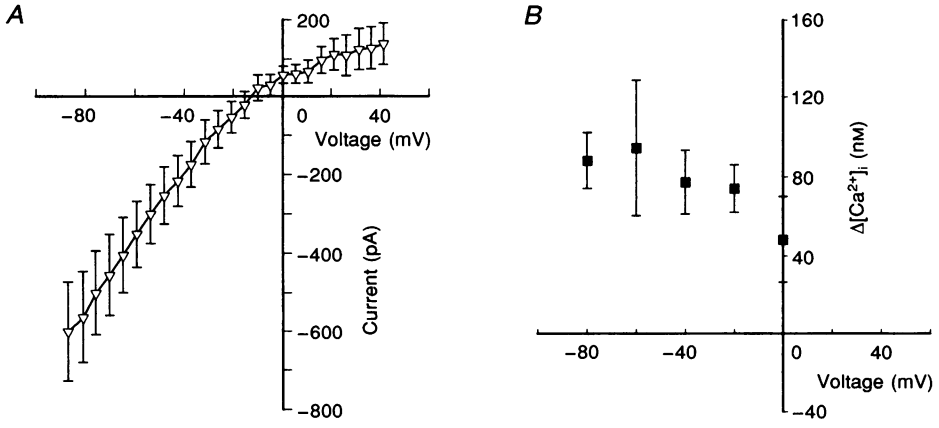

Figure 2. Influence of transmembrane potential on ATP-evoked currents and Ca^{2+} responses

A, the currents were measured during a continuous perfusion of 10 μM ATP and subjected to a depolarizing voltage ramp protocol from holding potential of −80 to 40 mV (1·2 mV ms^{-1}). Current values were measured every 5 mV and are means ± S.E.M. from eight different IHCs. The current–voltage plot of ATP-evoked currents demonstrated strong inward rectification at potentials below 0 mV, with a mean reversal potential of −11 ± 6 mV. *B*, because of their large run-down after successive ATP applications, the Ca^{2+} responses at each holding potential were obtained from different cells and measured at the peak following first ATP application (10 μM). Values are means ± S.E.M. ($n = 3$–10 cells). The ATP-evoked Ca^{2+} responses did not show a significant dependence on membrane potential (in *A* and *B* the cells were recorded using the conventional whole-cell recording technique).

potentials and exhibited a strong rectification at potentials above 0 mV. The currents showed a mean reversal potential of −11 ± 6 mV ($n = 8$). This reversal potential was not significantly displaced when we replaced KCl with potassium gluconate in our recording intracellular solution suggesting that a Cl^- conductance was not activated during ATP application. A reversal potential near 0 mV suggested that the ATP-sensitive channels in IHCs were permeable to more than one cationic species (probably Na^+, K^+ and Ca^{2+}) and resembled ATP-operated non-selective cationic channels described in OHCs (Nakagawa *et al.* 1990).

Because of the rapid run-down of the ATP-evoked Ca^{2+} responses after several ATP exposures, the $[Ca^{2+}]$–V relationship was constructed from the first ATP-evoked Ca^{2+} responses measured in different voltage clamped cells.

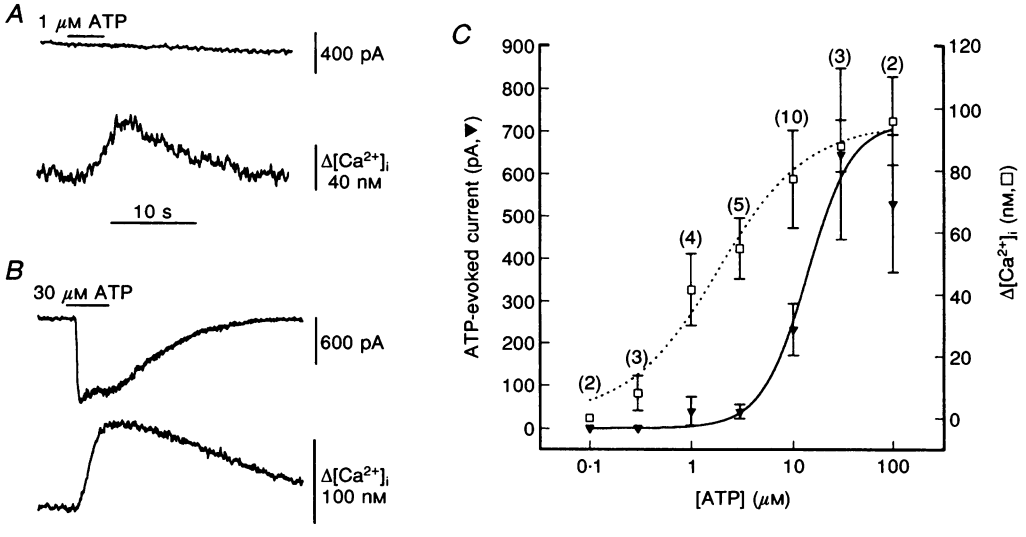

Figure 3. Comparative dose–response curves of ATP-evoked currents and Ca^{2+} responses

A and *B*, examples of simultaneous recordings of currents (upper traces) and Ca^{2+} responses (lower traces) evoked by 1 (*A*) and 30 μM (*B*) ATP in two different voltage clamped IHCs at −40 mV. The peak amplitudes of current and corresponding rise in $[Ca^{2+}]_i$, measured for each cell on first ATP application, are plotted in *C* for various ATP concentrations. The values are means ± S.E.M. measured from different cells. The data were best fitted with a sigmoidal curve with an EC_{50} of 1·8 ± 0·3 μM and Hill coefficient of 1·0 ± 0·1 for Ca^{2+} responses and an EC_{50} of 13·7 ± 3·0 and Hill coefficient of 2·0 ± 0·7 for current responses.

No significant difference in the amplitude of the Ca^{2+} responses was observed between cells clamped at various voltages between −80 and 0 mV (Fig. 2*B*). The results indicated that the ATP-induced Ca^{2+} signals were essentially due to Ca^{2+} release from intracellular stores not to Ca^{2+} influx since the amplitude was not affected by decreasing the transmembrane electrochemical driving force for Ca^{2+}.

Comparative dose–response curve of ATP-evoked currents and Ca^{2+} responses

Ca^{2+} responses could be observed at ATP concentrations as low as 0·3 and 1 μM while no significant effect on steady-state current was observed at such ATP concentrations ($n = 8$) (Fig. 3*A*). Concomitant Ca^{2+} signals and inward currents could only be recorded at ATP concentrations above 3 μM (Fig. 3*B*). The dose–response curves of current and Ca^{2+} response were constructed from the first ATP-evoked Ca^{2+} signals and the corresponding first ATP-activated inward currents of IHCs voltage clamped at −40 mV. The curves indicated a mean 50% effective concentration (EC_{50}) of 1·8 ± 0·3 and 13·7 ± 3·0 μM, respectively (Fig. 3*C*). The data were best fitted with sigmoidal curves with Hill coefficients of 1·0 ± 0·1 and 2·0 ± 0·7 for Ca^{2+} responses and ATP-evoked currents, respectively. Different EC_{50} and Hill coefficients between ATP-evoked current and Ca^{2+} responses suggested that two different P_2-purinergic receptors were involved in IHCs. Similar EC_{50} and Hill coefficient values were obtained for ATP-evoked currents when the dose–response curve was constructed with data obtained from the same IHCs stimulated by various ATP concentrations.

Comparative effects of extracellular Ca^{2+} on ATP-evoked currents and Ca^{2+} responses

As shown above, the ATP-evoked currents showed faster kinetics than Ca^{2+} signals in normal HBSS (1·25 mM $CaCl_2$) but when we looked in more detail, there was no significant difference in the onset of activation (Fig. 4*A*). The kinetic of the Ca^{2+} signals showed two different phases: a slow increase in the first seconds followed by a rapid second phase (Fig. 4*A*).

In 0 Ca_o^{2+}, the slow first phase of Ca^{2+} rise was not observed and a clear shift in latency of 3·7 ± 0·3 s ($n = 3$) could be measured between the onset of the ATP-evoked current and the onset of the Ca^{2+} responses (Fig. 4*B*). In the same cells, upon the third application of ATP in standard HBSS, the amplitude of the Ca^{2+} signals showed only a single slow phase with no delay in onset of activation with the current (Fig. 4*C*). These observations suggested that some Ca^{2+} influx may explain the primary slow rise in $[Ca^{2+}]_i$ during ATP stimulation.

The amplitude of the ATP-evoked current was not reduced in 0 Ca_o^{2+} conditions (Ca^{2+} replaced by Mg^{2+}, 5 mM EGTA was added to chelate residual free Ca^{2+}), but on the

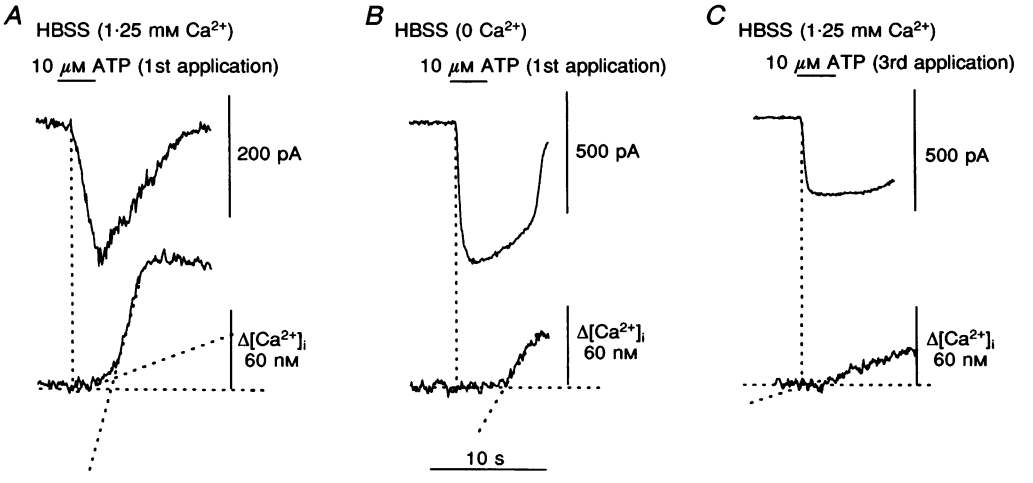

Figure 4. Onset of activation of ATP-evoked Ca^{2+} responses

A, example of ATP-evoked current (upper trace) and Ca^{2+} response (lower trace) from a voltage clamped IHC at −40 mV in HBSS. Note that the rise in $[Ca^{2+}]_i$ presented a biphasic kinetic and its onset was concomitant with the inward current. *B* and *C* show typical recordings from the same IHC during a first application of ATP (10 μM) in zero calcium HBSS and after a third ATP application in normal HBSS. Note that in the absence of extracellular Ca^{2+} (*B*), the Ca^{2+} signal was maintained but showed a significant delay (3·7 ± 0·3 s; $n = 3$) compared with the current response. This delayed Ca^{2+} signal is probably due to Ca^{2+} release from intracellular stores. The Ca^{2+} signal presented a strong desensitization in amplitude at the third ATP application (*C*) but its onset was concomitant with the current response. This residual Ca^{2+} signal is probably due to Ca^{2+} influx. Furthermore, note that the amplitude of the current response was larger and its deactivation faster in the absence of extracellular Ca^{2+}.

contrary was increased by 100% compared with control values (Figs 4*B*, *C* and 5). This suggested that extracellular calcium reduces the conductance of the ATP-activated channels. Indeed, raising extracellular Ca^{2+} concentration to 3 and 10 mM (keeping Na^+ concentration constant) from 1·25 mM reversibly reduced the ATP-evoked currents by 70 and 90%, respectively, compared with control values. We calculated that free ATP concentration in HBSS changed from 430 nM to 260 and 100 nM when adding 3 and 10 mM $CaCl_2$, respectively. However, this effect seemed not to be due to a change in the concentration of free ATP. In separate experiments in which EGTA was used to vary the concentration of free ATP, there was no difference in the amplitude of the ATP-evoked currents. Indeed, in 0 Ca_o^{2+} conditions in the presence or absence of 5 mM EGTA and for 10 μM total ATP, the free ATP concentration was calculated to increase from 399 to 4210 nM, respectively. This suggested that the ATP salt form is the potent activator of IHCs ionotropic receptors. This fits well with the activation of P_{2X}-receptors where ATP salt seems to be the actual ligand, contrary to P_{2Z}-receptors (ATP forming pores) where it is ATP^{4-} (see Dubyack & El-Moatassim, 1993).

However, the amplitude of the ATP-evoked Ca^{2+} responses was not significantly affected by reducing or increasing extracellular Ca^{2+} (Fig. 5*B*). Taken together, these results suggested that the Ca^{2+} responses were essentially derived from mobilization of intracellular stores via the activation of a metabotropic receptor, but some Ca^{2+} influx via ionotropic receptors may also participate in the early rise in $[Ca^{2+}]_i$ during ATP application.

Effects of heparin

The effects of heparin, a putative blocker of the $InsP_3$ receptors (Ghosh, Eis, Mullaney, Evert & Gill, 1988), was tested on the ATP-evoked responses. Heparin (1 mg ml^{-1}) was intracellularly dialysed via the patch pipette using whole-cell recording conditions. The cells were stimulated by ATP 5 min after rupturing the patch membrane, allowing equilibrium of the pipette solution with the cell cytosol. The ATP-evoked currents showed no significant difference from controls during successive applications of 10 μM ATP (Fig. 6). On the contrary, the corresponding ATP-evoked Ca^{2+} responses were significantly reduced to 32% ($n = 8$) compared with control cells without heparin (Fig. 6). The Ca^{2+} ionophore ionomycin was added as a

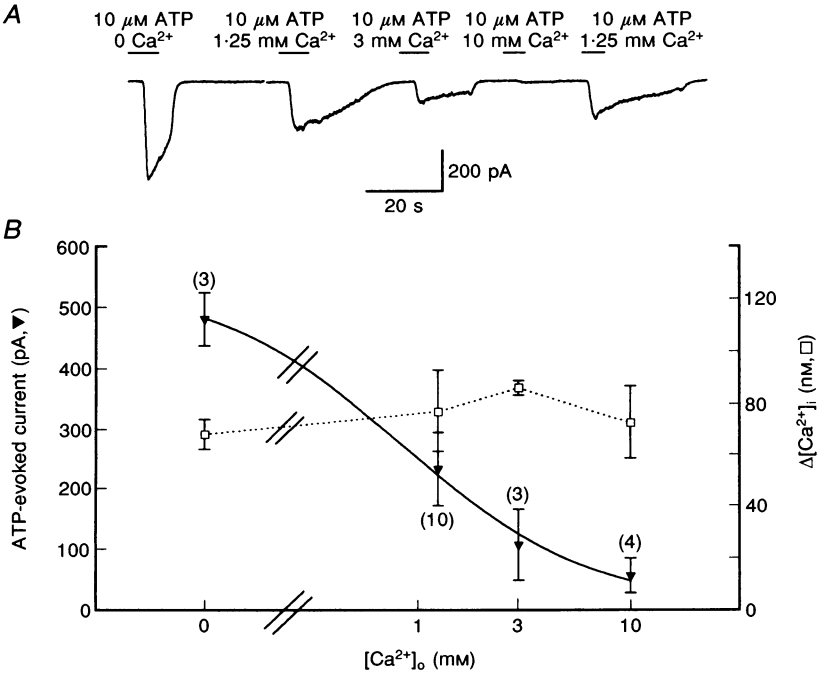

Figure 5. Increasing extracellular Ca^{2+} decreased the amplitude of the ATP-evoked current

A, example of successive ATP-evoked currents from an IHC voltage clamped at −40 mV in various extracellular Ca^{2+} concentrations. Zero extracellular calcium conditions were obtained by applying ATP dissolved in Ca^{2+}-free HBSS (Mg^{2+} substituted for Ca^{2+}) supplemented with 5 mM EGTA. *B*, the peak amplitudes of ATP-evoked current and corresponding Ca^{2+} response were measured at the first ATP application. Values are means ± S.E.M. measured from different cells placed in various extracellular Ca^{2+} concentrations (0, 1·25, 3 and 10 mM). The IHCs were voltage clamped at −40 mV. Note that there was no significant variation in the amplitude of the Ca^{2+} responses indicating that the participation of a Ca^{2+} influx was very small compared with Ca^{2+} release from intracellular stores.

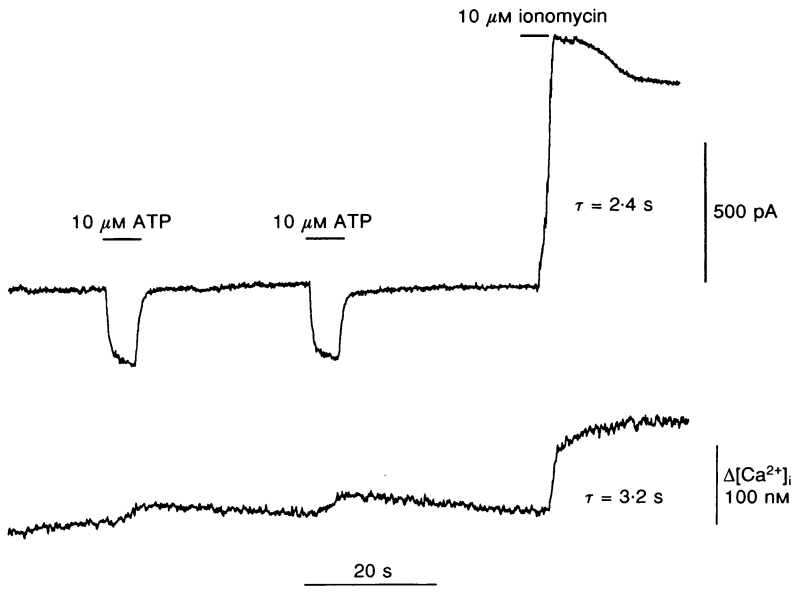

Figure 6. Intracellular heparin largely reduced the ATP-evoked Ca^{2+} response

The figure shows a simultaneous recording of current (upper trace) and $[Ca^{2+}]_i$ (lower trace) during sequential applications of ATP and ionomycin in an IHC voltage clamped at −40 mV. The cell was intracellularly dialysed via the patch pipette with heparin (1 mg ml^{-1}). Note that the Ca^{2+} responses produced by ATP were very small while the amplitude of the current responses appeared unaffected. Ionomycin (10 μM) was used as a control to show that $[Ca^{2+}]_i$ could be increased in these cells. The ionomycin-induced Ca^{2+} signal was concomitant with an outward current, presumably a Ca^{2+}-activated K^+ conductance.

control at the end of the experiments in four cells to check that heparin did not abolish or interfere with the indo-1 responses. The subsequent addition of ionomycin increased $[Ca^{2+}]_i$ and concomitantly activated an outward current. The effects of heparin suggested that the rise in $[Ca^{2+}]_i$ upon ATP application might be coupled to the phosphotidylinositol cascade via the activation of P_2-purinergic metabotropic receptors. Interestingly, the activation of the outward current, concomitant to the ionomycin-evoked rise in $[Ca^{2+}]_i$, presumably corresponded to the Ca^{2+}-activated K^+ currents previously described in IHCs (Dulon *et al.* 1995).

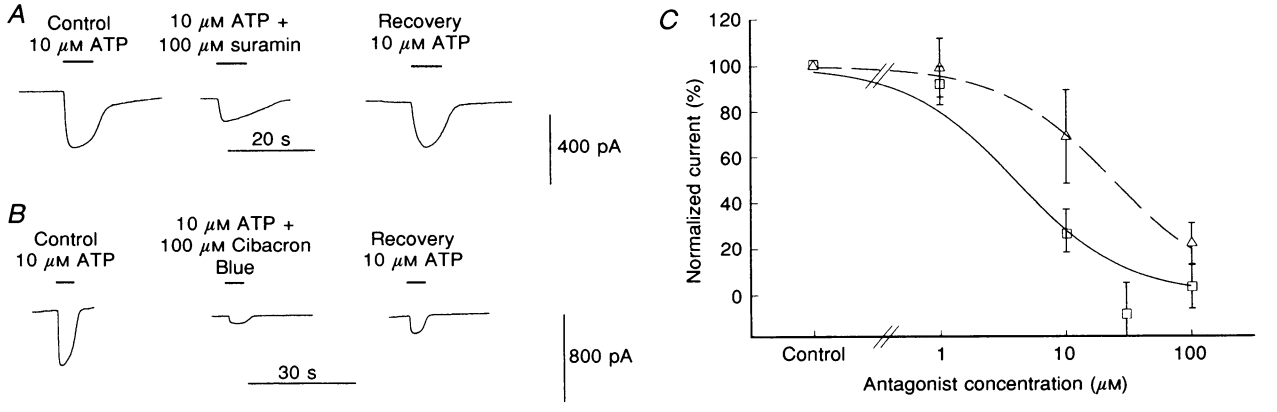

Figure 7. Inhibition of ATP-evoked currents by the P_2-purinergic antagonists suramin and Cibacron Blue

The figure shows ATP-evoked currents reversibly blocked by suramin (*A*) and by Cibacron Blue (*B*) in two different IHCs voltage clamped at −40 mV. The inhibition curves for suramin (△) and Ciberon Blue (□) are shown in *C*. For each cell, the amplitudes of currents induced in the presence of various concentration of antagonist were normalized to the current obtained with 10 μM ATP before antagonist application. Values are means ± S.E.M. of 5 cells for each antagonist. The data were best fitted with a sigmoid curve (Hill slope, −1) having an IC_{50} of 24 ± 3 and 4 ± 1 μM for suramin and Cibacron Blue, respectively.

Effects of P_2-purinergic receptor antagonists on ATP-evoked currents

Suramin and Cibacron Blue (one of the isomers of Reactive Blue) are well known as P_2-purinergic antagonists, blocking ionotropic, as well as metabotropic, receptors (Dunn & Blakely, 1988; Hoyle, Knight & Burnstock, 1990). The ATP-evoked currents in IHCs voltage clamped at −40 mV were reversibly blocked by suramin or Cibacron Blue in a dose-dependent manner (Fig. 7). The lowest concentration tested at which these drugs were significantly effective was 10 μM, blocking 32 ± 21 ($n = 5$) and 75 ± 10% ($n = 5$) of the ATP-evoked current for suramin and Cibacron Blue, respectively. The blocking effects of 100 μM suramin and 100 μM Cibacron Blue with partial recovery are shown in Fig. 7*A* and *B*. The 50% inhibitory concentration (IC_{50}) was calculated to be 24 ± 3 and 4 ± 1 μM for suramin and Cibacron Blue, respectively.

These purinergic antagonist molecules interfered with our measurements of intracellular calcium using single excitation wavelength (380 nm) and dual emission (405 nm/480 nm). Perfusing extracellular suramin or Cibacron Blue even at moderate concentrations (30 μM; data not shown) artefactually increased the emission fluorescence ratio (F_{405}/F_{480}) of indo-1, so under our experimental conditions we could not determine the effects of these drugs on the ATP-evoked Ca^{2+} responses.

Location of ionotropic channel

In order to identify the cellular location of the ATP-gated ionotropic receptors, ATP was pressure puffed via a pipette with a small tip diameter (1–2 μm) and placed near the cell (10 μm) at three different sites (Fig. 8, representative of four different IHCs tested). The largest currents with shortest latencies were observed when ATP was applied toward the apex (Fig. 8*A*). We did not observe significant differences between puffs directed towards the stereocilia (endolymphatic site) or the lateral side of the cuticular plate. Our data, in agreement with Housley *et al.* (1993), suggest that the ionotropic receptors are located towards the upper part of the IHCs, similarly to what has been shown for OHCs (Housley, Greenwood & Ashmore, 1992), but we cannot say that they are exclusively facing the endolymph.

DISCUSSION

We have shown that extracellular ATP activated a non-specific cationic conductance and evoked concomitant Ca^{2+} responses in IHCs. These Ca^{2+} responses, mainly due to Ca^{2+} release from intracellular stores, showed the following characteristics compared with the inward currents: (i) a slower kinetic of activation with a longer onset latency; (ii) a strong run-down after several ATP applications; (iii) no dependence on transmembrane membrane potential; (iv) an eightfold lower apparent K_d with a different Hill coefficient; (v) peak amplitude remained unchanged in zero extracellular Ca^{2+} conditions while inward currents were increased; and (vi) blocked by intracellular heparin. All these results suggested the presence of two subtypes of P_2-purinergic receptor in IHCs: metabotropic and ionotropic receptors. Our data suggested that these two ATP receptors

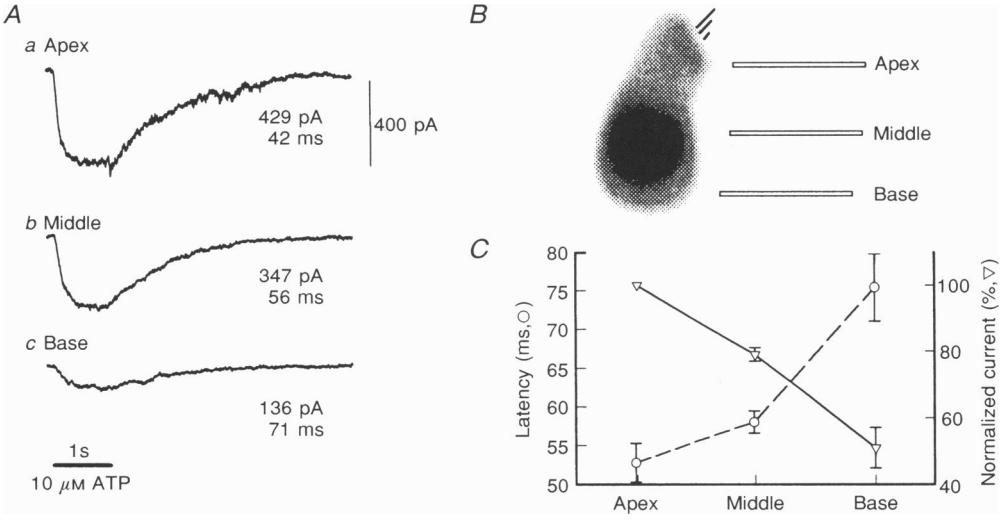

Figure 8. Location of ATP-gated ionotropic receptors

A, example of currents when ATP was sequentially applied to different regions of an IHC. The peak amplitudes and onset latencies in response to ATP (10 μM) are given below each current trace. The cell was voltage clamped at −40 mV. Acquisition rate was 150 Hz. The different locations of the tip of the puff pressure pipette containing ATP are drawn in *B*. The largest current and shortest latency were observed with the pipette placed at the apex of the cell (region *a*). The latencies and ATP-evoked currents are plotted in *C*. Each point represents means ± S.E.M. of 4 cells. The current amplitudes were normalized to the response measured when ATP was applied to the apex for each cell. These results are consistent with localization of the ATP-gated ionotropic receptors in the apical region of the IHCs.

might produce opposite electrical responses *in vivo*: the metabotropic receptors leading to hyperpolarization via activation of Ca^{2+}-activated K^+ currents (Dulon *et al.* 1995) and the ionotropic receptors leading primarily to depolarization.

There are two possibilities for the respective localization of these two types of receptor. First, they could be co-localized in the apical regions of the cells since the fastest and largest current responses were obtained in this area. Therefore, at low concentrations of extracellular ATP (below 3 μM) the main electrical response of IHCs should be hyperpolarization from rest due to activation of Ca^{2+}-activated K^+ conductance. At higher extracellular ATP concentrations, the ionotropic receptors would, on the contrary, produce a fast depolarization followed by a slower repolarization due to Ca^{2+}-activated K^+ conductance. Since IHCs are believed to function as presynaptic terminals releasing glutamate upon sound stimulation, one can speculate that ATP would differently modulate receptor potentials and neurotransmission at submicromolar or at micromolar concentrations.

A second possibility was that the ionotropic and metabotropic receptors are located at different sites on the cell surface. The ionotropic receptors seemed to be placed in the apical region of the IHCs, confirming the results of Housley *et al.* (1993). We do not know where the ATP receptors linked to Ca^{2+} mobilization are located but one can speculate that they are localized in the synaptic region on the other side of the cell. These metabotropic receptors could possibly be co-localized with Ca^{2+}-activated K^+ channels and Ca^{2+} channels. These latter channels have been suggested to be simultaneously present at active zones facing the afferent nerve terminals (Roberts, 1993; Issa & Hudspeth, 1994). Therefore, in this separated configuration, the metabotropic receptors would primarily influence neurotransmission while ionotropic receptors would influence mechanotransduction.

A consistent observation was the irreversibility of the run-down of the ATP-evoked Ca^{2+} signals. This could be due to: (i) metabotropic receptors being desensitized, so requiring an additional extracellular factor to return to their original active state, or (ii) the intracellular messenger receptor being desensitized. An alternative could be that the Ca^{2+} stores are not refilled after a first stimulation because isolated IHCs *in vitro* are in a low energy state. However, even when we added 1 mM ATP to our internal solution the run-down process was not significantly reduced (data not shown). The run-down was not due to use of 1 mM BAPTA as the intracellular Ca^{2+} buffer because run-down was also observed under perforated patch conditions in which the natural cell Ca^{2+} buffer is preserved. This irreversible run-down of ATP-evoked Ca^{2+} signals was not peculiar to IHCs since it was also observed in isolated supporting cells of the organ of Corti, the Deiters cells (Dulon *et al.* 1993).

On the contrary, the ATP-evoked non-specific cationic currents did not show significant run-down but were dramatically reduced when rising extracellular Ca^{2+} and were increased in zero Ca^{2+} solutions. A similar increase in ATP-evoked current was reported in IHCs after removal of divalent cations by Mockett, Housley & Thorne (1994). Furthermore, identical effects of extracellular Ca^{2+} have been reported on ATP-gated non-selective cationic channels in phaeochromocytoma cells and cultured neurons (Nakazawa, Fujimori, Takanaka & Inoue, 1990; Fieber & Adams, 1991). One possible explanation was that the permeability of the ATP-operated channels to Ca^{2+} ions is low, as suggested by our simultaneous measurements of current and $[Ca^{2+}]_i$, and that Ca^{2+} ions could compete at the channel mouth with other cations resulting in a partial obstruction of the channels.

The presence of purinergic receptors has been suggested in other cell types of the cochlea, in particular in the other sensory hair cell types, the OHCs (Ashmore & Ohmori, 1990; Nakagawa *et al.* 1990) and in supporting cells such as the Deiters and Hensen cells (Dulon *et al.* 1993). The EC_{50} of ATP-evoked currents of IHCs were similar to OHCs but IHCs showed a Hill coefficient of 2 instead of 1 (Nakagawa *et al.* 1990). Our results indicated two binding sites for ATP in IHCs as previously reported in other neuronal P_{2X}-receptors (Furakawa, Ishihashi & Akaike, 1994; Brake *et al.* 1994).

On the other hand, the affinity of the metabotropic receptors for ATP in IHCs was similar to that in Deiters cells (Dulon *et al.* 1993) but twentyfold higher than that reported in OHCs (Nilles *et al.* 1994). These results suggested that different subtypes of purinergic receptor might be expressed in IHCs and OHCs. The physiological significance of these differences between IHCs and OHCs is difficult to explain but could be related to their different role in cochlear transduction, the IHCs being the primary transducers and the OHCs being active mechanical amplifiers (for review see Dallos, 1992). It is interesting to note that recent studies using perilymphatic perfusion of ATP agonists have suggested that ATP could act on different cell types in the cochlea (Kujawa *et al.* 1994).

Despite the biological effects of extracellular ATP reported in the cochlea, the possible sources for extracellular ATP are still unknown. Since extracellular ATP is known to be rapidly hydrolysed into adenosine by ectoATPase and ectophosphatase, usually present at the cell surfaces of different tissues and cells, the sources of ATP should be located near their target cell receptors in the cochlea. Adenosine, released when ATP is hydrolysed by ATPase, is well known for mediating various biological responses (Gordon, 1986) via the activation of P_1-purinergic receptors. Such adenosine receptors did not appear to be present in IHCs since we could not observe any significant currents or Ca^{2+} responses with 10 μM adenosine (data not

shown) which is in agreement with previous results (Dulon *et al.* 1991*a*). Extracellular ATP, believed to be one of the major neurotransmitters in the CNS (Edwards & Gibb, 1992; Evans, Derkach & Surprenant, 1992) has been shown to be co-released in millimolar concentrations with noradrenaline and acetylcholine in non-purinergic synapses (Westfall, Sedaa, Shinozuka, Bjur & Buxton, 1990). In the cochlea, ATP could also be co-released with putative transmitters such as ACh and glutamate at the efferent and afferent nerve terminals, respectively (for review see Eybalin, 1993). It has been shown that there are many efferent synapses at the basal pole of the guinea-pig IHCs (Hashimoto, Kimura & Takasaka, 1990) and these synapses could also be good candidates for releasing ATP. Another possible source of ATP in the cochlea could come from cytolytic release from damaged cells during hypoxia, overstimulation or chemical intoxication as suggested in many other cell types (Dubyak & El-Moatassim, 1993). The later possibility fits well with the existence of purinergic receptors in supporting cells which are generally recognized to have very sparse synaptic innervation.

In conclusion, the present study has shown that both ATP-activated metabotropic receptors and ionotropic receptors are co-expressed in IHCs. Therefore, extracellular ATP could lead to concentration-dependent opposite effects in IHCs of the cochlea, leading to depolarization via the activation of ionotropic receptors or hyperpolarization via the activation of metabotropic receptors. The determination of the respective cell localization of these receptors and the sources of extracellular ATP now appear to be the principal challenge over the next few years to understanding the physiological roles of ATP in the cochlea.

Ashmore, J. F. & Ohmori, H. (1990). Control of intracellular calcium by ATP in isolated outer hair cells of the guinea-pig cochlea. *Journal of Physiology* **428**, 109–131.

Brake, A. J., Wagenbach, M. J. & Julius, D. (1994). New structural motif for ligand-gated ion channels defined by an ionotropic ATP receptor. *Nature* **371**, 519–523.

Burnstock, G. (1978). A basis for distinguishing two types of purinergic receptors. In *Cell Membrane Receptors for Drugs and Hormones: A Multidisciplinary Approach*, ed. Straub, R. W. & Bolis, L., pp. 107–118. Raven Press. New York.

Dallos, P. (1986). Neurobiology of cochlear inner and outer hair cells: intracellular recordings. *Hearing Research* **22**, 185–198.

Dallos, P. (1992). The active cochlea. *Journal of Neuroscience* **12**, 4575–4585.

Dubyak, G. R. & El-Moatassim, C. (1993). Signal transduction via P2-purinergic receptors for extracellular ATP and other nucleotides. *American Journal of Physiology* **265**, C577–606.

Dulon, D., Moataz, R. & Mollard, P. (1993). Characterization of Ca^{2+} signals generated by extracellular nucleotides in supporting cells of the organ of corti. *Cell Calcium* **14**, 245–254.

Dulon, D., Mollard, P. & Aran, J.-M. (1991*a*). Extracellular ATP elevates cytosolic Ca^{2+} in cochlear inner hair cells. *NeuroReport* **2**, 69–72.

Dulon, D., Sugasawa, M., Blanchet, C. & Erostegui, C. (1995). Direct measurements of Ca^{2+}-activated K^+ currents in inner hair cells of the guinea-pig cochlea using photolabile Ca^{2+} chelators. *Pflügers Archiv* **430**, 365–373.

Dulon, D., Zajic, G. & Schacht, J. (1991*b*). Differential motile response of isolated inner and outer hair cells to stimulation by potassium and calcium ions. *Hearing Research* **52**, 225–232.

Dunn, P. M. & Blakely, A. G. H. (1988). Suramin: a reversible P2-purinoceptor antagonist in mouse vas deferens. *British Journal of Pharmacology* **93**, 243–245.

Edwards, F. A. & Gibb, A. J. (1992). ATP – a fast neurotransmitter. *Federation of European Biochemical Societies* **325**, 86–89.

Evans, R. J., Derkach, J. V. & Surprenant, A. (1992). ATP mediated fast synaptic transmission in mammalian neurons. *Nature* **357**, 503–505.

Eybalin, M. (1993). Neurotransmitters and neuromodulators of the mammalian cochlea. *Physiological Reviews* **73**, 309–373.

Fieber, L. A. & Adams, D. J. (1991). Adenosine triphosphate-evoked currents in cultured neurons dissociated from rat parasympathetic cardiac ganglia. *Journal of Physiology* **434**, 239–256.

Furukawa, K., Ishihashi, H. & Akaike, N. (1994). ATP-induced inward current in neurons freshly dissociated from the tuberomammillary nucleus. *Journal of Neurophysiology* **71**, 868–873.

Ghosh, T. K., Eis, P. S., Mullaney, J. M., Evert, C. L. & Gill, D. L. (1988). Competitive, reversible and potent antagonism of inositol 1,4,5-triphosphate-activated calcium release by heparin. *Journal of Biological Chemistry* **263**, 11075–11079.

Gitter, A. H. & Zenner, H. P. (1990). The cell potential of isolated inner hair cells *in vitro*. *Hearing Research* **45**, 87–94.

Gordon, J. L. (1986). Extracellular ATP: effects, sources and fate. *Biochemical Journal* **233**, 309–319.

Hamill, O. P., Marty, A., Neher, E., Sakmann, B. & Sigworth, F. J. (1981). Improved patch-clamp techniques for high-resolution current recording from cells and cell-free membrane patches. *Pflügers Archiv* **391**, 85–100.

Hara, N., Ichinose, M., Sawada, M. & Maeno, T. (1990). Extracellular ATP activated Ca^{2+}-dependent K^+ conductance via Ca^{2+} influx in mouse macrophages. *Comparative Biochemistry and Physiology* **97A**, 417–421.

Hashimoto, S., Kimura, R. S. & Takasaka, T. (1990). Computer-aided three-dimensional reconstruction of the inner hair cell and their nerve endings in guinea pig cochlea. *Acta Otolaryngologica* **109**, 235–244.

Horn, R. & Marty, A. (1989). Muscarinic activation of ionic currents measured by a new whole-cell recording method. *Journal of General Physiology* **92**, 145–159.

Housley, G. D., Greenwood, D. & Ashmore, J. F. (1992). Localization of cholinergic and purinergic receptors on outer hair cells from guinea-pig cochlea. *Proceedings of the Royal Society* B **249**, 265–273.

Housley, G. D., Greenwood, D., Mockett, B. G., Muñoz, D. J. B. & Thorne, P. R. (1993). Differential actions of ATP-activated conductances in outer and inner hair cells isolated from the guinea-pig organ of Corti: A humoral purinergic influence on cochlear function. In *Biophysics of Hair Cell Sensory Systems*, ed. Duifhuis, H., Horst, J. W., van Dijk, P. & van Netten, S. M., pp 116–123. World Scientific, Singapore.

HOYLE, G. H. V., KNIGHT, G. E. & BURNSTOCK, G. (1990). Suramin antagonizes responses to P2-purinoceptor agonists and purinergic nerve stimulation in guinea-pig urinary bladder and taenia coli. *British Journal of Pharmacology* **99**, 617–621.

ISSA, N. P. & HUDSPETH, A. J. (1994). Clustering of Ca^{2+} channels and Ca^{2+}-activated K^+ channels at fluorescently labeled presynaptic zones of hair cells. *Proceedings of the National Academy of Sciences of the USA* **91**, 7578–7582.

KIANG, N. Y. S., RHO, J. M., NORTHROP, J. M., LIBERMAN, M. C. & RYUGO, D. K. (1982). Hair-cell innervation by spiral ganglion cells in adult cats. *Science* **217**, 175–177.

KROS, C. J. & CRAWFORD, A. C. (1990). Potassium currents in inner hair cells isolated from the guinea-pig cochlea. *Journal of Physiology* **421**, 263–291.

KUJAWA, S. G., EROSTEGUI, C., FALLON, M., CRIST, J. & BOBBIN, R. P. (1994). Effects of adenosine 5′-triphosphate and related agonists on cochlear function. *Hearing Research* **76**, 87–100.

MARTY, A. & NEHER, E. (1985). Potassium channels in cultured bovine adrenal chromaffin cells. *Journal of Physiology* **367**, 117–141.

MOCKETT, B. G., HOUSLEY, G. D. & THORNE, P. R. (1994). Fluorescence imaging of extracellular purinergic receptor sites and putative ecto-ATPases sites on isolated cochlear hair cells. *Journal of Neuroscience* **14**, 6992–7007.

MURASE, K., RYU, P. D. & RANDIC, M. (1989). Excitatory and inhibitory amino acids and peptide-induced responses in acutely isolated rat spinal dorsal horn neurons. *Neuroscience Letters* **103**, 56–63.

NAKAGAWA, T., AKAIKE, N., KIMITUKI, T., KOMUNE, S. & ARIMA, T. (1990). ATP-induced current in isolated outer hair cells of guinea pig cochlea. *Journal of Neurophysiology* **63**, 1068–1074.

NAKAZAWA, K., FUJIMORI, K., TAKANAKA, A. & INOUE, K. (1990). An ATP-activated conductance in phenochromocytoma cells and its suppression by extracellular calcium. *Journal of Physiology* **428**, 257–272.

NILLES, R., JÄRLEBARK, L., ZENNER, H. P. & HEILBRONN, E. (1994). ATP-induced cytoplasmic $[Ca^{2+}]$ increases in isolated cochlear outer hair cells. Involved receptor and channel mechanisms *Hearing Research* **73**, 27–34.

ROBERTS, W. M. (1993). Spatial calcium buffering in saccular hair cells. *Nature* **363**, 74–76.

UENO, S., ISHIBASHI, H. & AKAIKE, N. (1992). Perforated patch method reveals extracellular ATP-induced K^+ conductance in dissociated rat nucleus solitarii neurons. *Brain Research* **597**, 176–179.

VALERA, S., HUSSY, N., EVANS, R. J., ADDAMI, N., NORTH, R. A., SURPRENANT, A. & BUELL, G. (1994). A new class of ligand -gated ion channel defined by P_{2X} receptor for extracellular ATP. *Nature* **371**, 516–519.

WESTFALL, D. P., SEDAA, K. O., SHINOZUKA, K., BJUR, R. A. & BUXTON, I. L. (1990). ATP as a cotransmitter. *Annals of the New York Academy of Sciences* **603**, 300–310.

Acknowledgements

This work was supported by the Institut National Scientifique d'Etude et Recherche Medicale (INSERM). Masashi Sugasawa MD, PhD, is a research fellow from the Department of Otorhinolaryngology (University of Tokyo). We wish to thank the Fondation pour la Recherche Médicale (FRM, Paris, France) for its financial support of Carlos Erostegui.

Received 24 March 1995; accepted 7 August 1995.